Biogeochemistry (2018) 140:341–357
https://doi.org/10.1007/s10533-018-0495-1

Soil C:N:P stoichiometry responds to vegetation change from grassland to woodland

Yong Zhou · Thomas W. Boutton · X. Ben Wu

Received: 9 November 2017 / Accepted: 4 September 2018 / Published online: 11 September 2018

Abstract Woody encroachment has been a major land cover change in dryland ecosystems during the past century. While numerous studies have demonstrated strong effects of woody encroachment on soil carbon (C), nitrogen (N), and phosphorus (P) storage, far less is known about the plasticity of soil C:N:P stoichiometry in response to woody encroachment. We assessed landscape-scale patterns of spatial heterogeneity in soil C:N:P ratios throughout a 1.2 m soil profile in a region where grassland is being replaced by a diverse assemblage of subtropical woody plants dominated by *Prosopis glandulosa*, an N_2-fixing tree. Woody species had leaf and fine root C:N:P ratios significantly different from grasses. Variation in soil C:N ratios in both horizontal and vertical planes was remarkably smaller than that of soil N:P and C:P ratios. Spatial patterns of soil C:N ratio throughout the profile were not strongly related to vegetation cover. In contrast, spatial patterns of soil N:P and C:P ratios displayed a strong resemblance to that of vegetation cover throughout the soil profile. Within the uppermost soil layer (0–5 cm), soil N:P and C:P ratios were higher underneath woody patches while lower within the grassland; however, this pattern was reversed in subsurface soils (15–120 cm). These results indicate a complex response of soil C:N:P stoichiometry to vegetation change, which could have important implications for understanding C, N, and P interactions and nutrient limitations in dryland ecosystems.

Keywords Soil C:N:P stoichiometry · Woody encroachment · Pattern of spatial heterogeneity · Landscape scale · Soil profile · Subtropical savanna

Introduction

The consistent C:N:P stoichiometry in the ocean (Redfield ratio, Redfield 1958) has prompted decades of research in ecological stoichiometry that has addressed the balance of C, N, and P between organisms and substrates in ecological interactions, and now serves as a powerful tool for understanding the cycling of these elements in terrestrial ecosystems (Sterner and Elser 2002). Despite relatively constrained C:N:P ratios in soils, soil microbial biomass, forest foliage and litter at the global scale (McGroddy

Responsible Editor: Asmeret Asefaw Berhe.

Electronic supplementary material The online version of this article (https://doi.org/10.1007/s10533-018-0495-1) contains supplementary material, which is available to authorized users.

Y. Zhou (✉) · T. W. Boutton · X. B. Wu
Department of Ecosystem Science and Management, Texas A&M University, College Station, TX 77843-2126, USA
e-mail: zhouyong1222@tamu.edu

et al. 2004; Cleveland and Liptzin 2007), C:N:P stoichiometric variability frequently occurs at smaller spatial scales, especially in response to changes in species composition and/or dominance (Sardans et al. 2012; Sistla and Schimel 2012), nutrient additions (Güsewell 2004; Sardans et al. 2012; Xiao et al. 2015), and climate change (Elser et al. 2010; Dijkstra et al. 2012; Yue et al. 2017).

A notable example of species dominance shift is the globally widespread phenomenon of woody plant encroachment into grasslands, savannas, and other arid and semiarid ecosystems (Stevens et al. 2017). Although the exact cause remains unclear, livestock grazing, fire suppression, rising atmospheric CO_2 concentration, and/or climate change are likely drivers of this extensive land cover change (Scholes and Archer 1997; Morgan et al. 2007; Van Auken 2009; Wigley et al. 2010; Brunelle et al. 2014; Devine et al. 2017). This vegetation change is often associated with major changes in the structural and functional attributes of the dominant plant species that could potentially modify the stoichiometric characteristics of plant and soils where encroachment occurs. For example, the C:N:P stoichiometry in plant tissues has been shown to vary between life-forms such as grasses, forbs, and shrubs (Reich and Oleksyn 2004; Peng et al. 2011; Di Palo and Fornara 2017). In addition, many of the tree species encroaching into grasslands around the world (e.g. *Prosopis* and *Acacia*) are capable of symbiotic N-fixation, thereby adding N to the ecosystem (Boutton and Liao 2010; Sitters et al. 2013; Soper et al. 2015). Lastly, woody species generally have deep root systems (Jackson et al. 1996; Schenk and Jackson 2002; Zhou et al. 2018a) which enable them to acquire P from subsurface soils that are inaccessible to the more shallow-rooted grasses (Kantola 2012; Sitters et al. 2013; Blaser et al. 2014; Zhou et al. 2018b). Since there is growing evidence that plant functional traits serve as important drivers of soil biological processes (Bardgett and Wardle 2010), the alteration of C:N:P stoichiometry in plant tissues during vegetation change from grass to woody plant dominance is expected to have corresponding effects on soil C:N:P stoichiometry (Zechmeister-Boltenstern et al. 2015).

However, previous studies assessing the consequences of woody encroachment on soil biogeochemical cycling have focused almost exclusively on pool sizes and flux rates of soil C and N (Hibbard et al. 2001; Wheeler et al. 2007; Boutton and Liao 2010), and few studies have characterized effects on soil P cycling (Kantola 2012; Sitters et al. 2013; Blaser et al. 2014; Zhou et al. 2018b). Therefore, little is known about the plasticity of soil C:N:P stoichiometry in response to woody encroachment. Among the studies which have reported soil C:N ratio as a soil characteristic, some have shown no net change following woody encroachment (Hibbard et al. 2001; Liao et al. 2006; Wheeler et al. 2007), some have reported a reduction (Geesing et al. 2000; McCulley and Jackson 2012), while others have reported an increase (Springsteen et al. 2010; Creamer et al. 2011; Kantola 2012). Additionally, Kantola (2012) found that soil N:P and C:P ratios increased linearly with stand age of woody patches in a subtropical savanna encroached by *Prosopis glandulosa*, while no significant changes in soil N:P and C:P ratios were reported in other studies (Sitters et al. 2013; Blaser et al. 2014). Reasons for these discrepancies remain unclear but may be related to the identity of encroaching woody species (e.g. N_2-fixer vs. non-N_2-fixer), soil nutrient status (e.g. nutrient poor vs. nutrient rich soils), and/or land use history (Geesing et al. 2000; Hibbard et al. 2001; Springsteen et al. 2010; McCulley and Jackson 2012; Kantola 2012; Sitters et al. 2013; Blaser et al. 2014). It is worth noting that the aforementioned studies on soil C:N, N:P, and/or C:P ratios examined only surface soils (top 15 cm). Given that recent studies have shown that woody encroachment can have a significant impact on subsurface soil C, N and P storage (Jackson et al. 2002; McCulley and Jackson 2012; Chiti et al. 2017; Zhou et al. 2017a, 2018a), this represents a potential knowledge gap regarding how C:N:P stoichiometry response to woody encroachment might evolve throughout the entire soil profile.

There is increasing recognition of the need for application of quantitative spatial methods for the study of ecosystem processes (Ettema and Wardle 2002), especially for soil biogeochemical processes in dryland ecosystems where patchiness of vegetation may favor the development of islands of fertility (Schlesinger et al. 1996). Previous studies have demonstrated that woody encroachment into grasslands has dramatically increased spatial variability and uncertainty of soil attributes (Throop and Archer 2008; Bai et al. 2009; Liu et al. 2011; Zhou et al. 2017a), making it difficult to generalize results from the ecosystem to the landscape scale (Zhou et al.

2017b). Despite this, most empirical studies on soil C:N:P stoichiometry have exclusively focused on the ecosystem scale, and far less is known about landscape-scale patterns of spatial heterogeneity in soil C:N, N:P, and C:P ratios in arid and semiarid ecosystems, especially those undergoing vegetation change from grassland to woodland. This lack of understanding of spatial patterns of soil C:N:P stoichiometry may limit our ability to identify and quantify the biotic and abiotic factors by which they are driven.

The primary objective of this study is to assess the responses of landscape-scale spatial patterns of soil C:N:P stoichiometry throughout the soil profile to woody encroachment. To accomplish this, we took spatially-explicit soil cores to a depth of 120 cm throughout a 160 m × 100 m subtropical savanna landscape which has undergone encroachment by *Prosopis glandulosa* and other woody species during the past century in southern Texas, USA. Our specific objectives were to (1) investigate changes in plant leaf and fine root C:N, N:P, and C:P ratios during vegetation change from grassland to woodland; (2) quantify patterns of spatial heterogeneity in soil C:N, N:P, and C:P ratios across this landscape and throughout the soil profile; and (3) identify biotic and abiotic factors responsible for the variation in soil C:N, N:P, and C:P ratios in 3-dimensional soil space.

Methods and materials

Study site

This study was conducted at the Texas A&M AgriLife La Copita Research Area (27°40′N, 98°12′W) located in the eastern Rio Grande Plains, Texas, USA. Climate is subtropical with mean annual temperature and precipitation of 22.4 °C and 680 mm, respectively. Rainfall peaks generally occur in May and September. Elevation ranges from 75 m to 90 m above sea level. The landscape consists of nearly level uplands that grade gently (1–3% slope) to lower-lying drainage woodlands and playas. Upland soils are sandy loam with a continuous subsurface argillic horizon (*Typic Argiustolls*); however, non-argillic inclusions (*Typic Haplustepts*) are also present (Archer 1995).

It has been well documented that upland vegetation at this site was once dominated primarily by C_4 grasses, and that woody encroachment has occurred over the past century in response to livestock grazing and fire suppression (Archer 1995; Boutton et al. 1998). The increasing abundance of woody plants is initiated by the colonization of *Prosopis glandulosa*, an N_2-fixing tree legume (Zitzer et al. 1996). Once established, these *P. glandulosa* trees then serve as nurse plants to facilitate the recruitment and establishment of other woody species beneath their canopies to form discrete clusters (generally < 100 m^2) (Archer 1995; Bai et al. 2012). If discrete clusters occur on soils with non-argillic inclusions, they expand laterally and eventually coalesce to form large groves (generally > 100 m^2) (Archer 1995; Bai et al. 2012; Zhou et al. 2017b). Although groves are largely constrained to those portions of the landscape where the argillic horizon is absent, they will sometimes encroach slightly beyond the non-argillic boundaries onto areas where the argillic horizon is present, albeit at reduced rates of expansion (Bai et al. 2009; Zhou et al. 2017b). More details about spatial relationships between the distribution of groves and non-argillic inclusions can be found in Zhou et al. (2017b). Thus, the current vegetation pattern on upland portions of this landscape can be characterized as a two-phase pattern of woody patches scattered throughout a grassland matrix (Whittaker et al. 1979). The grassland matrix is co-dominated by C_4 grasses and C_3 forbs. Clusters and groves are dominated by *P. glandulosa* trees, though the age and size of *P. glandulosa* trees in clusters are significant smaller than those in groves (Boutton et al. 1998). Understory shrub/tree species composition is similar in both clusters and groves. A list of the dominant plant species in grasslands, clusters, and groves can be found in Appendix S1.

Field sampling and lab analyses

On an upland portion of this study site, a 160 m × 100 m landscape was established and subdivided into 10 m × 10 m grid cells in January 2002 (Fig. 1) (Bai et al. 2009; Liu et al. 2011). The X, Y coordinates of each corner of each grid cell were assigned using a GPS unit (Pathfinder Pro XRS, Trimble Navigation Ltd., Sunnyvale, CA, USA) based on the UTM coordinate system (14 North, WGS 1984). Two sampling points were randomly selected within each 10 m × 10 m grid cell in July 2014,

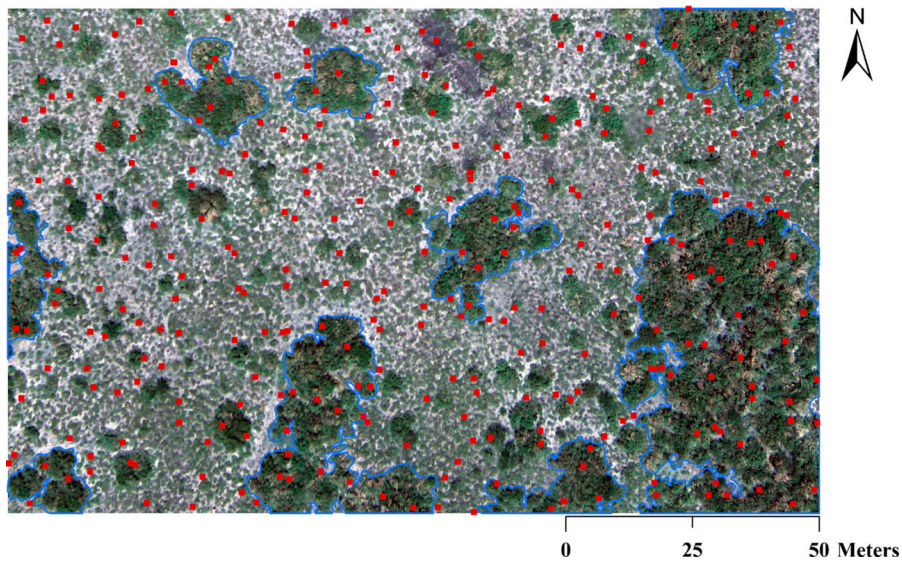

Fig. 1 Aerial photograph of the 160 × 100 m landscape. Red squares indicate locations of the 320 random soil sampling points. Green patches are woody clusters and groves, while light grey areas indicate open grasslands. Canopy edges of groves are highlighted with blue lines. Modified Zhou et al. 2017a, b. (Color figure can be viewed in the online issue)

yielding a total of 320 sampling points across this landscape (Fig. 1). Distances from each sampling point to two georeferenced corners were recorded. The landscape element present at each sample point was categorized as grassland (n = 200), cluster (n = 41) or grove (n = 79) based on vegetation type and the canopy size of woody patches. At each sampling point, two adjacent soil cores (2.8 cm in diameter and 120 cm in length) were collected using the PN150 JMC Environmentalist's Subsoil Probe (Clements Associates Inc., Newton, IA, USA). Soil cores were subsequently divided into 6 depth increments (i.e. 0–5, 5–15, 15–30, 30–50, 50–80, and 80–120 cm). A color-infrared aerial photograph (6 cm × 6 cm resolution) of this landscape was acquired and georeferenced with ground control points in July 2015, and then digitized to produce a classified vegetation map. Leaf and fine root tissues of each plant species occurring on this landscape were collected in September 2016 (Appendix S1).

One soil core was used to estimate fine (2 < mm) and coarse (> 2 mm) root biomass by washing through sieves. Retrieved roots were oven-dried (65 °C for 48 h) for biomass determination. The other soil core was air-dried and subsequently passed through a 2 mm sieve to remove coarse organic fragments. No gravel was present in soil samples. Sieved soil samples were used to determine soil pH on a 1: 2 (10 g soil: 20 mL 0.01 mol/L $CaCl_2$) mixture using a glass electrode, and soil texture using the hydrometer method.

An aliquot of soil that passed through the 2 mm sieve was dried at 65 °C for 48 h, and then pulverized in a centrifugal mill (Angstrom, Inc., Belleville, MI, USA). Collected leaf and fine root tissues were carefully washed, dried, and also pulverized. Total C and total N concentrations of pulverized soil, leaf and fine root tissue samples were determined by dry combustion using a Costech ECS 4010 elemental analyzer (Costech Analytical Technologies Inc., Valencia, CA, USA). Organic C concentration of pulverized soil samples was determined using the same combustion system, but soil samples were pretreated with HCl vapor in a desiccator for 8 h to remove carbonates (Harris et al. 2001), and dried. Inorganic C concentration of soil samples was calculated by subtracting organic C concentration from total C concentration. The lithium fusion method was used to extract total P from pulverized soil, and from leaf and fine root tissue samples (Lajtha et al. 1999). More details can be found in Zhou et al. (2017b). The P concentration in extracted solutions was determined by using the molybdenum blue colorimetry method (Murphy and Riley 1962) using a Spectronic $20D^+$ spectrophotometer (Thermo Fisher Scientific, Inc., Waltham, MA, USA).

Data analyses

C:N, N:P, and C:P ratios were calculated on a mass basis. Datasets that were not normally distributed were $\log_{10}$-transformed to improve normality. Soil C:N, N P, and C:P ratios of different landscape elements (i.e. grassland, cluster, and grove) for each soil depth increment were compared using mixed models. Spatial autocorrelation of variables was taken into account as a spatial covariance for adjustment in mixed models (Littell et al. 2006). One-way ANOVA was used to compare leaf and fine root C:N, N:P, and C:P ratios for different plant life forms. A cutoff value of $p < 0.05$ was used to indicate significant differences. Post-hoc comparisons of these variables were conducted with Tukey's test. All statistical analyses were performed using JMP Pro 12.0 (SAS Institute Inc., Cary, NC, USA).

Across this landscape, some non-argillic inclusions within the grassland matrix are still not occupied by groves (Zhou et al. 2017b). This allows us to address the potential effect of the subsurface argillic horizon on soil C:N:P stoichiometry. We subdivided soil cores obtained within the grassland matrix into those taken where the argillic horizon was present versus those taken where the argillic horizon was absent using soil diagnostics for the higher categories as outlined in USDA Soil Taxonomy (Soil Survey Staff 1999; Zhou et al. 2018a). One-way ANOVA was performed to compare C:N, N:P, and C:P ratios of soils sampled from argillic versus non-argillic portions of the grassland.

A sample variogram fitted with a variogram model was constructed to quantify the spatial structure for soil C:N, N:P, and C:P ratios within each depth increment based on 320 random soil samples using R statistical software (R Development Core Team 2014) (Appendix S2, S3, S4, S5, and S6). Ordinary kriging based on parameters from variogram models and values of 320 random soil samples was used for spatial interpolation. Kriged maps of soil C:N, N:P, and C:P ratios across this landscape and throughout the soil profile were generated accordingly using ArcMap 10.2.2 (ESRI, Redlands, CA, USA). Lacunarity, a scale-dependent measurement of spatial heterogeneity or the "gappiness" of a landscape structure (Plotnick et al. 1996), was used to quantify the spatial heterogeneity of soil C:N, N:P, and C:P ratios across this landscape and throughout the soil profile. Lacunarity analyses were performed based on kriged maps using R statistical software. Lacunarity curves, plotted as the natural log transformations of lacunarity values $\Lambda(r)$ against box sizes (r) in meter, were created to visualize the spatial heterogeneity of soil C:N, N:P, and C:P ratios at different spatial scales (i.e. box sizes), with a higher value of lacunarity indicating a more heterogeneous distribution pattern across the landscape.

Correlations between soil C:N, N:P, and C:P ratios, fine root density (kg m^{-3}), soil clay (%), silt (%), pH, and inorganic carbon concentration (g C kg^{-1} soil) across this landscape and throughout the soil profile were assessed using Pearson's correlation coefficients and a modified t test for testing significances. The modified t-test adjusts the degrees of freedom based on the extent of spatial autocorrelation in the datasets (Dutilleul et al. 1993). Descriptive statistics for fine root density, soil clay, silt, pH and inorganic carbon concentration have been presented elsewhere (Zhou et al. 2017a, b). Datasets were $\log_{10}$-transformed prior to the analysis of correlations using PASSaGE version 2 (Rosenberg and Anderson 2011).

Results

C:N:P stoichiometry of leaves and fine roots

Across this landscape, woody species (both non N_2- and N_2-fixers, hereafter) had significantly lower mean C:N ratios in leaf tissues than grasses (Fig. 2a). Although not significant, woody species had lower mean C:P but higher mean N:P ratios in leaf tissues than grasses (Fig. 2a). Forbs had mean C:N, N:P, and C:P ratios comparable to non N_2-fixing woody species (Fig. 2a). Woody species had significantly lower mean C:N and C:P ratios in fine root tissues than grasses, and non-N_2-fixing woody species had significantly higher N:P ratios than grasses (Fig. 2b). Although not significant, woody species had lower mean C:N and C:P but higher mean N:P ratios in fine root tissues than forbs (Fig. 2b).

Spatial patterns of soil C:N:P stoichiometry

Soil mean C:N, N:P, and C:P ratios all decreased with soil depth, but the decreases in N:P and C:P ratios were considerably larger than those for C:N ratio (Table 1).

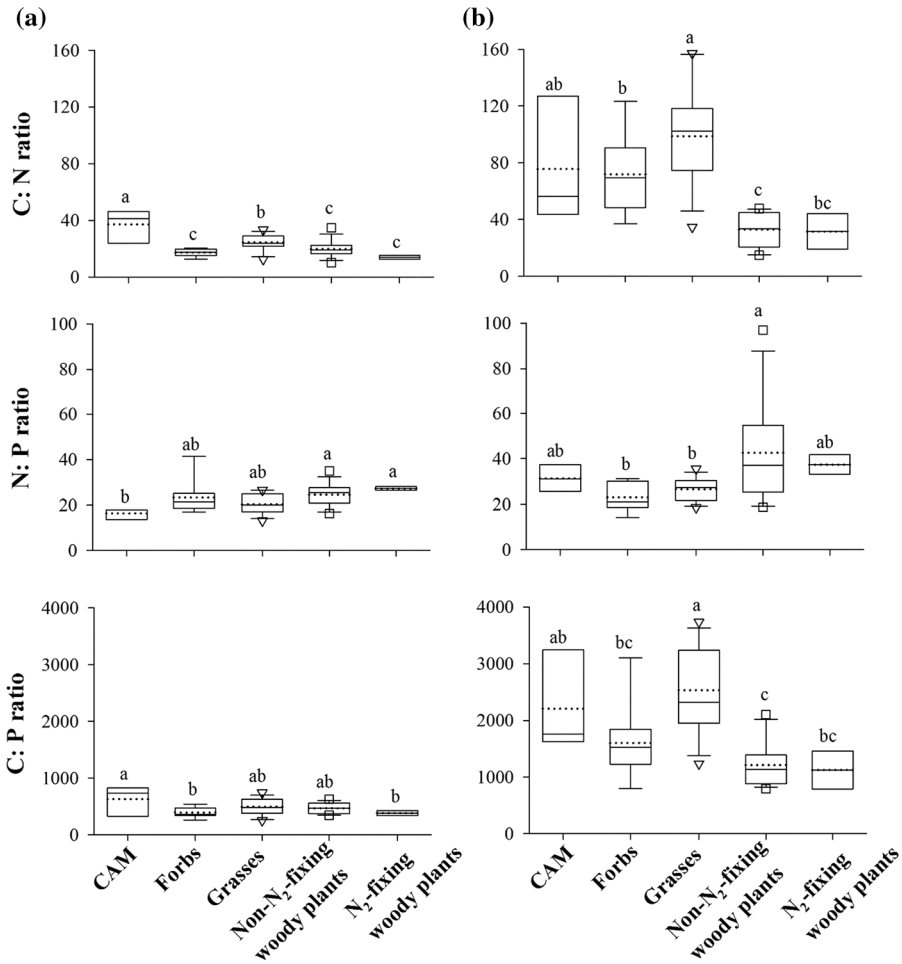

Fig. 2 C:N, N:P, and C:P ratios of leaf (**a**) and fine root (**b**) tissues for different plant life-forms occurring on this 160 m × 100 m landscape. The box plots summarize the distribution of points for each variable of each plant life-form. The central box shows the inter-quartile range, median (horizontal solid line in the box), and mean (horizontal dotted line in the box). Lower and upper error bars indicate 10th and 90th percentiles, and points above and below the error bars are individuals above the 90th or below the 10th percentiles. Significant differences ($p < 0.05$) are indicated with different letters. CAM, crassulacean acid metabolism species, n = 3; Forbs, n = 9; Grasses, n = 13; Non-N_2-fixing woody species, n = 13; N_2-fixing woody species, n = 2. Values for individual species are provided in Appendix S1

For example, mean soil C:N ratio decreased from 10.3 in the 0–5 cm depth increment to 8.2 in the 80–120 cm depth increment, whereas the N:P ratio decreased from 9.7 to 3.8 and the C:P ratio decreased from 101.3 to 31.6 (Table 1). Variation in soil N:P and C:P ratios across the landscape was generally about 2–6 times higher than that for the C:N ratio throughout the entire soil profile, as evidenced by coefficients of variation (CVs) (Table 1).

Soil C:N, N:P, and C:P ratios of grasslands on non-argillic inclusions were not significantly different from those on the argillic horizon throughout the entire soil profile (Fig. 3), excluding the possible influence of pre-existing differences in subsurface soil texture on soil C:N:P stoichiometry. Following woody plant encroachment into grasslands, groves had significantly higher soil C:N ratios than grasslands throughout the soil profile, except in the 5–15 cm depth increment (Table 2). Groves and clusters had significantly higher soil N:P and C:P ratios than grasslands in the 0–5 cm depth increment; however, groves had significantly lower soil N:P and C:P ratios than both grasslands and clusters throughout the 15–120 cm portion of the soil profile (Table 2).

Visual comparison of the classified vegetation map of this landscape and kriged maps of soil C:N ratios at each depth throughout the soil profile revealed that spatial patterns of soil C:N ratios were almost irrelevant to those of vegetation cover (Fig. 4a and b). In contrast, spatial patterns of soil N:P and C:P ratios throughout the soil profile displayed strong resemblance to the spatial distribution of woody patches, except in the 5–15 cm depth increment (Fig. 4c and d). Soil N:P and C:P ratios were the highest at the centers of woody patches, decreased towards the woody patch/grassland boundary, and

Table 1 Descriptive statistics for soil C:N, N:P, and C:P ratios throughout the soil profile. CV is coefficient of variation

	0–5 cm	5–15 cm	15–30 cm	30–50 cm	50–80 cm	80–120 cm
C:N ratio						
Mean	10.34	9.79	10.02	9.67	8.86	8.23
Median	10.27	9.77	10.00	8.60	8.80	8.31
Minimum	8.31	8.20	7.83	8.20	8.27	5.79
Maximum	16.41	11.90	12.64	12.71	10.97	10.71
CV	0.06	0.06	0.07	0.07	0.06	0.09
Skewness	2.74	0.54	− 0.05	0.87	0.92	− 0.18
N:P ratio						
Mean	9.71	7.48	6.50	5.78	4.77	3.84
Median	8.48	7.46	6.59	6.02	4.98	3.87
Minimum	4.45	4.55	2.83	2.75	2.26	1.92
Maximum	26.88	15.03	9.35	8.52	6.33	6.14
CV	0.35	0.14	0.16	0.21	0.18	0.14
Skewness	2.07	1.19	− 0.55	− 0.32	− 0.71	− 0.05
C:P ratio						
Mean	101.31	73.28	65.09	55.72	42.01	31.55
Median	86.77	72.36	66.39	57.41	42.96	31.54
Minimum	47.18	39.74	27.36	27.62	22.60	12.33
Maximum	319.43	161.78	91.52	83.69	59.37	63.70
CV	0.40	0.16	0.18	0.21	0.16	0.15
Skewness	2.32	1.57	− 0.51	− 0.33	− 0.41	0.68

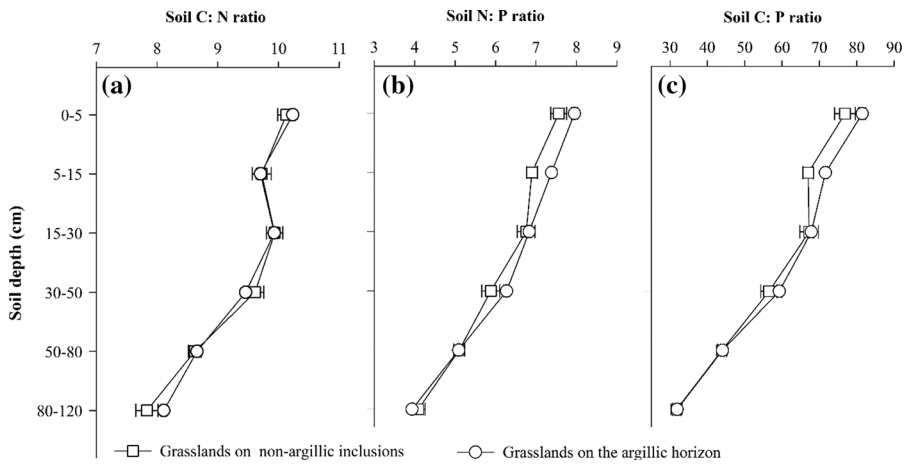

Fig. 3 Soil C:N (**a**), N:P (**b**), and C:P (**c**) ratios of samples from the grassland matrix occurring on the argillic horizon vs. on non-argillic inclusions. Number of samples: grasslands on non-argillic inclusions, 17; grasslands on the argillic horizon, 183. There were no significant differences in soil C:N, N:P, or C:P ratios between samples from the argillic horizon and non-argillic inclusion throughout the soil profile

reached lowest values within the grassland matrix in the 0-5 cm depth increment (Fig. 4c and d). However, these patterns were reversed in deeper portions of the soil profile (15–120 cm), with lower soil N:P and C:P ratios underneath groves compared to the remnant grassland matrix (Fig. 4c and d).

Lacunarity analyses indicated that spatial heterogeneities of soil C:N ratio for all depth increments (Fig. 5a) were remarkably lower than those of soil N:P

Table 2 Mean and standard error of soil C:N, N:P and C:P ratios for different landscape element across this 160 m × 100 m landscape and throughout the soil profile

Parameter	Landscape element	0–5 cm	5–15 cm	15–30 cm	30–50 cm	50–80 cm	80–120 cm
C:N ratio							
	Grassland	10.23 ± 0.04^{b}	9.70 ± 0.04^{a}	9.93 ± 0.05^{b}	9.47 ± 0.04^{b}	8.65 ± 0.03^{c}	8.09 ± 0.05^{b}
	Cluster	10.62 ± 0.17^{a}	9.88 ± 0.08^{a}	10.23 ± 0.12^{a}	9.97 ± 0.10^{a}	8.99 ± 0.07^{b}	8.26 ± 0.14^{b}
	Grove	10.48 ± 0.07^{a}	9.95 ± 0.06^{a}	10.13 ± 0.08^{ab}	10.02 ± 0.08^{a}	9.31 ± 0.07^{a}	8.58 ± 0.07^{a}
N:P ratio							
	Grassland	7.92 ± 0.07^{b}	7.34 ± 0.05^{b}	6.82 ± 0.05^{a}	6.24 ± 0.07^{a}	5.09 ± 0.04^{a}	3.95 ± 0.03^{a}
	Cluster	12.22 ± 0.51^{a}	8.61 ± 0.22^{a}	6.99 ± 0.14^{a}	6.09 ± 0.16^{a}	5.02 ± 0.12^{a}	4.04 ± 0.09^{a}
	Grove	12.96 ± 0.47^{a}	7.25 ± 0.14^{b}	5.42 ± 0.12^{b}	4.47 ± 0.12^{b}	3.83 ± 0.10^{b}	3.48 ± 0.07^{b}
C:P ratio							
	Grassland	81.08 ± 0.89^{b}	71.20 ± 0.53^{b}	67.76 ± 0.61^{a}	59.02 ± 0.64^{a}	44.03 ± 0.35^{a}	31.90 ± 0.30^{a}
	Cluster	131.32 ± 7.08^{a}	85.19 ± 2.47^{a}	71.49 ± 1.71^{a}	60.42 ± 1.52^{a}	44.98 ± 1.02^{a}	33.49 ± 0.92^{a}
	Grove	136.98 ± 5.51^{a}	72.38 ± 1.57^{b}	55.02 ± 1.35^{b}	44.93 ± 1.30^{b}	35.37 ± 0.80^{b}	29.66 ± 0.56^{b}

Significant differences ($p < 0.05$) between means in landscape element are indicated with different superscript letters. Number of samples: grassland = 200, cluster = 41, and grove = 79

and C:P ratios (Fig. 5b and c) across this landscape. Additionally, the highest spatial heterogeneity for soil N:P and C:P ratios was observed in the 0–5 cm depth increment (Fig. 5b and c). Results from lacunarity analysis were consistent with variation in C:N, N:P, and C:P ratios as indicated by CVs across this landscape (Table 1).

Correlations between soil C:N:P stoichiometry, vegetation, and soil physicochemical factors

Soil C:N was significantly and positively correlated with fine root density throughout the soil profile except in the 15–30 cm depth increment; soil C:P and N:P ratios were significantly and positively correlated with fine root density in the 0–5 and 5–15 cm depth increments, but were negatively correlated in the 15–30, 30–50, and 50–80 cm increments (Table 3).

Soil C:N ratio was significantly and negatively correlated with clay content only in the 30–50 and 50–80 cm depth increments, whereas soil N:P and C:P ratios were significantly and positively correlated with clay in these two depth increments (Table 3). Soil N:P and C:P ratios were significantly and negatively correlated with soil pH in the 15–30, 30–50, and 50–80 cm soil depth increments (Table 3). Meanwhile, soil N:P and C:P ratios were significantly and negatively correlated in the 5–15, 15–30, 30–50, and 50–80 cm depth increments (Table 3).

Discussion

Changes in plant leaf and fine root C:N:P stoichiometry in response to woody encroachment

Vegetation change from grassland to woodland has dramatically altered plant leaf and fine root C:N:P stoichiometry across this landscape (Fig. 2). Lower C:N and C:P ratios in leaf and fine root tissues of woody species compared to grasses may be ascribed to the fact that C concentrations of woody species are relatively comparable to those of grasses, while N and P concentrations are much higher in the woody species (Zhou et al. 2018c). There are three potential explanations for this: (1) the dominant tree (i.e. *P. glandulosa*) in woody patches across this landscape is a legume and capable of symbiotic N_2-fixation (Zitzer et al. 1996; Boutton and Liao 2010; Soper et al. 2015); (2) *P. glandulosa* and other woody species have deeper root systems than herbaceous species (grasses, forbs) that dominate these grasslands (Watts 1993; Boutton et al. 1999), allowing them to access deep soil N and P located beyond the reach of other

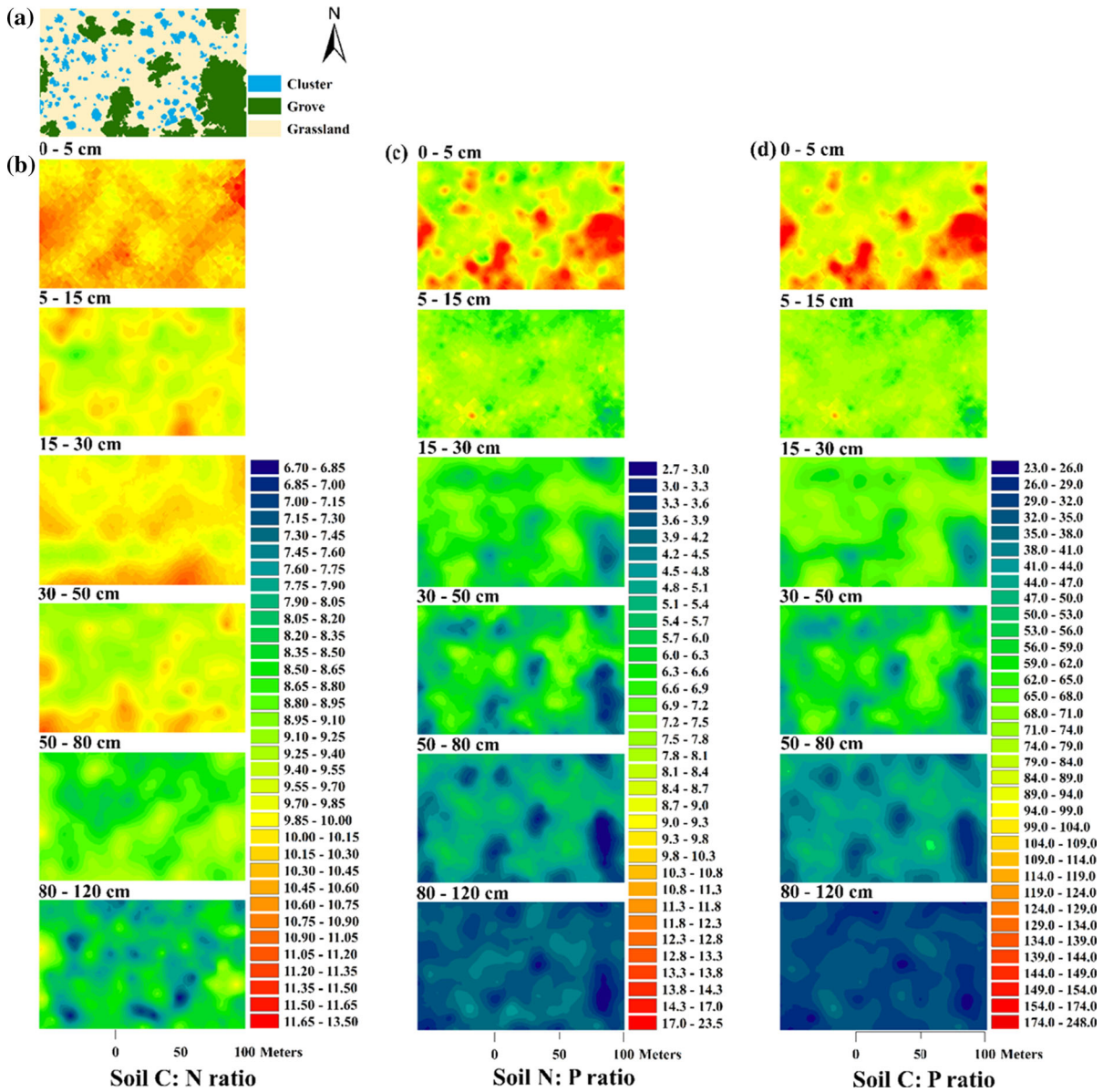

Fig. 4 Classified vegetation map (**a**) and kriged maps of soil C:N (**b**), N:P (**c**), and C:P (**d**) ratios based on 320 random sampling points across this 160 m × 100 m landscape and throughout the soil profile. Note that the scale is different for each elemental ratio. (Color figure can be viewed in the online issue)

plant species (Zhou et al. 2017b); and (3) soils beneath N_2-fixers generally have higher phosphatase enzyme activity than non N_2-fixers (Houlton et al. 2008; Boutton et al. 2009; Blaser et al. 2014; Png et al. 2017), enabling mineralization of organic P into plant available forms (Kantola 2012). Additional N and P acquired through these mechanisms eventually enrich soils beneath woody plant canopies via litterfall and root turnover (Schlesinger et al. 1996). Relatively N- and P-rich soils underneath woody patches compared to grasslands favor higher leaf and root N and P concentrations, thus lower C:N and C:P ratios in woody species (Zechmeister-Boltenstern et al. 2015).

N: P ratios of terrestrial plant species have been extensively studied as indicators of N or P limitation (Koerselman and Meuleman 1996; Güsewell 2004;

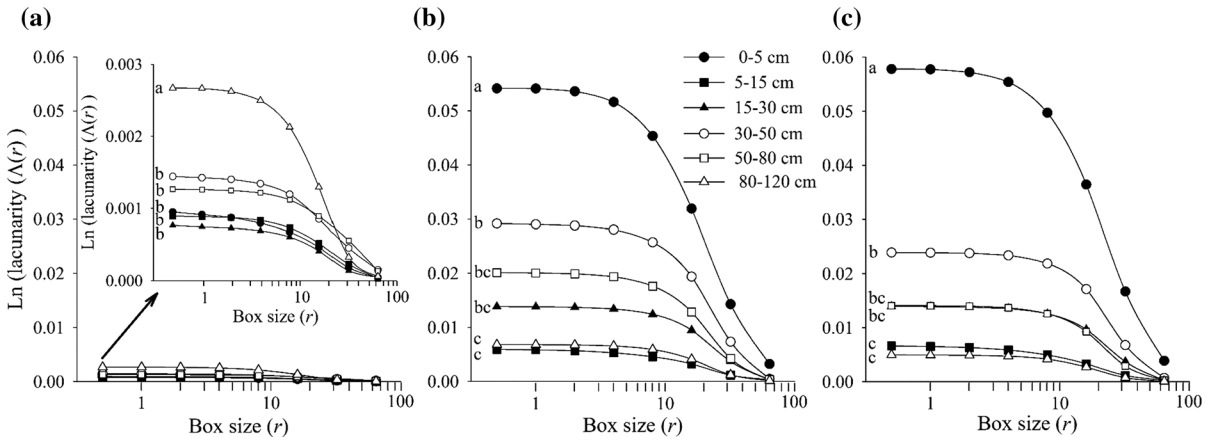

Fig. 5 Lacunarity curves for soil C:N (**a**), N:P (**b**), and C:P (**c**) ratios across this l60 m × 100 m landscape and throughout the soil profile. Significant differences ($p < 0.05$) are indicated with different letters

Han et al. 2005; Reich and Oleksyn 2004; Yuan et al. 2011). Individual measurements of plant N:P ratios range from approximately 1–100 (Güsewell 2004), but the average for terrestrial plant species is approximately 12–14 for leaves (Elser et al. 2000; Reich and Oleksyn 2004) and approximately 14–24 for roots depending on root size and status (i.e. live or dead) (Yuan et al. 2011). Our N:P ratios for leaves of all collected species are considerably higher than these aforementioned averages (Fig. 2), ranging from 16.4 for CAM species to 27.2 for N_2-fixing woody species (Fig. 2). It has been proposed that leaf N:P ratios > 16 indicate P limitation (Koerselman and Meuleman 1996; Güsewell 2004; Han et al. 2005), suggesting that plant species occurring on this landscape are more likely limited by P rather than N. In addition, woody plants (both N_2-fixing and non-N_2-fixing, n = 15) had higher mean N:P ratios in leaves (24.8 vs. 20.5) and fine roots (41.9 vs. 26.5) compared to grasses (Appendix S1), further suggesting that soil N might be relatively more available than P following woody plant encroachment since the dominant *P. glandulosa* and a few other understory species are capable of biological N-fixation (Zitzer et al. 1996; Soper et al. 2015).

Soil C:N ratios change little in response to woody encroachment

The significant resorption of N and P during plant organ senescence results in nutrient-depleted litter (Aerts 1996; Güsewell 2004; Lü et al. 2012), thus increasing C:N and C:P ratios of litter compared to live tissues (McGroddy et al. 2004). For this reason, the C:N:P of live leaf and fine root tissues may not represent those of litter and senesced roots which are the primary sources of soil organic matter. However, during plant litter decomposition, microbial N- and P-use efficiencies are higher than their C-use efficiency (Myrold 2005; Mooshammer et al. 2014); thus, losses of substrate C as CO_2 are proportionally much greater than losses of N and P that might occur during the decay process. For this reason, the C:N:P stoichiometry of decomposing plant litter tends to converge toward that of soil organic matter and soil microbial biomass (Moore et al. 2011; Manzoni et al. 2010, 2012; Zechmeister-Boltenstern et al. 2015). For example, despite large variation in litter C:N:P stoichiometry (McGroddy et al. 2004), a well-constrained mean C:N:P ratio of 72:6:1 has been reported for surface soils (0–10 cm) at the global scale (Cleveland and Liptzin 2007). In this subtropical savanna, mean soil C:N:P ratios across this landscape range from 101:10:1 in the surface soil to 32:4:1 in deeper portions of the profile (Table 1). When categorized by landscape elements and compared to soil C:P and N:P ratios, however, the soil C:N ratio varied less among different depth increments (Table 1 and 2, Fig. 4) and also among different landscape elements (Table 2), suggesting that responses of soil C:N ratio to woody encroachment throughout the soil profile are more constrained than those of soil C:P and N:P ratios.

The small variation in the depth distribution of soil C:N ratio across this landscape agrees with studies in

Table 3 Pearson's correlation coefficients (r) showing relationships between soil C:N, N:P, and C:P ratios, fine root density (FRD), soil clay, silt, pH, and inorganic carbon (IC) throughout the soil profile

Characteristic	Soil N:P	Soil C:P	FRD	Soil clay	Soil silt	Soil pH	Soil IC
0–5 cm							
Soil C:N	0.40***	0.55***	0.17**	0.05	0.01	− 0.00	0.25**
Soil N:P		0.99***	0.73***	0.11	0.21	− 0.01	0.37**
Soil C:P			0.70***	0.11	0.19	− 0.01	0.38**
FRD				0.08	0.19	0.06	0.32**
Soil clay					0.50*	0.13	0.13
Soil silt						0.15*	0.21*
Soil pH							0.28**
5–15 cm							
Soil C:N	0.06	0.42***	0.18**	0.04	0.06	0.08	− 0.06
Soil N:P		0.93***	0.18**	− 0.03	− 0.05	− 0.01	− 0.25***
Soil C:P			0.23***	− 0.01	− 0.02	0.02	− 0.25***
FRD				0.07	0.36**	0.33**	0.34***
Soil clay					0.47*	0.14	0.10
Soil silt						0.29***	0.38***
Soil pH							0.41***
15–30 cm							
Soil C:N	0.03	0.39***	0.12	− 0.04	0.15*	0.06	− 0.23***
Soil N:P		0.93***	− 0.23**	− 0.02	− 0.37*	− 0.46***	− 0.59***
Soil C:P			− 0.17*	− 0.03	− 0.28**	− 0.40***	− 0.63***
FRD				0.03	0.24*	0.32***	0.37***
Soil clay					0.42*	0.04	0.13
Soil silt						0.42***	0.41***
Soil pH							0.46***
30–50 cm							
Soil C:N	− 0.26***	0.02	0.27***	− 0.29***	0.24	0.18*	0.20**
Soil N:P		0.96***	− 0.25***	0.45**	− 0.26	− 0.62***	− 0.75*
Soil C:P			− 0.18**	0.38**	− 0.20*	− 0.59*	− 0.72*
FRD				− 0.21**	0.06	0.24**	0.37**
Soil clay					0.16	− 0.24*	− 0.18*
Soil silt						0.40**	0.31*
Soil pH							0.63***
50–80 cm							
Soil C:N	− 0.54***	− 0.26***	0.37***	− 0.37***	− 0.06	0.30***	0.32***
Soil N:P		− 0.95***	− 0.46***	0.46***	0.02	− 0.52***	− 0.58***
Soil C:P			− 0.39***	0.39***	0.00	− 0.49***	− 0.55***
FRD				− 0.32***	− 0.03	0.28***	0.34***
Soil clay					0.38***	0.05	− 0.00
Soil silt						0.25*	0.18
Soil pH							0.78***
80–120 cm							
Soil C:N	− 0.23***	0.34***	0.25***	0.09	0.11	0.29***	0.39***
Soil N:P		0.84***	− 0.22***	0.35***	− 0.24***	− 0.15*	0.00
Soil C:P			− 0.07	0.39***	0.29***	0.02	0.22***

Table 3 continued

Characteristic	Soil N:P	Soil C:P	FRD	Soil clay	Soil silt	Soil pH	Soil IC
FRD				− 0.16*	− 0.15*	0.16*	0.06
Soil clay					− 0.66***	− 0.32***	0.45***
Soil silt						0.16	0.38***
Soil pH							0.41***

A modified T-test for correlation was used to test for significance

*$p < 0.05$, **$p < 0.01$, ***$p < 0.001$

other savanna ecosystems worldwide (Lilienfein et al. 2001; McCulley and Jackson; 2012; Coetsee et al. 2013; Dintwe et al.; 2015), and with results from regional and global syntheses (Batjes 1996; Tian et al. 2010). As soil C and N are biologically mineralized and stabilized together, soil C:N ratio is often used to indicate the degree of decomposition (McGill and Cole 1981; Batjes 1996). The slight decrease in soil C:N ratio throughout the profile is consistent with the fact that soil organic matter stored in deeper portions of the soil profile is older and has experienced a greater degree of microbial decomposition (Boutton et al. 1998).

Soils underneath woody patches (both clusters and groves) had slightly higher C:N ratios than those underneath grasslands throughout the soil profile, although these differences were not always significant (Table 2). There are two possible explanations. Firstly, soils underneath woody patches have higher litter and root inputs compared to remnant grasslands (Liu et al. 2010; Zhou et al. 2017a), potentially leading to a soil organic matter pool comprised largely of plant materials in the early stages of decomposition in the upper portion of the profile (Liao et al. 2006). Secondly, litter in wooded areas consists of more biochemically recalcitrant materials (particularly aliphatic biopolymers) which are less suitable as microbial substrates compared to litter in remnant grasslands (Liao et al. 2006; Filley et al. 2008). This more recalcitrant litter in wooded areas may decompose more slowly and lead to higher soil C:N ratios (McGill & Cole 1981; Batjes 1996).

Although woody patches had slightly higher soil C:N ratios than grasslands throughout the soil profile as discussed above (Table 2), spatial patterns of soil C:N did not strongly resemble spatial patterns of vegetation across this landscape (Fig. 4a and b). This is likely due to the fact that relative changes of soil C and N in response to woody encroachment in this subtropical savanna are strongly coupled (Zhou et al. 2018c), lessening the potential for soil C:N differences between woody patches and grasslands (Table 2), as reflected by the small effective size (Cohen's $d < 0.5$, data not shown) (Cohen 1988) and overall variation ($CV < 0.09$, Table 1). Given this small overall variation and our low intensity random sampling design (two random samples per 100 m^2), the maps of C:N ratio were likely reflective of low-magnitude, and possibly random, variations resulting from other or legacy processes within both woody and grassland patches. A more intensive sampling regime may have lessened random effects and yielded more refined and accurate spatial patterns of soil C:N ratio.

More flexible soil C:P and N:P ratios in response to woody encroachment

Our results indicate that responses of soil C:P and N:P ratios to woody encroachment were very similar (Fig. 4c, d, 5b, and c), as soil C:P and N:P ratios were highly correlated throughout the soil profile ($r > 0.80$, Table 3), reflecting the fact that soil C and N are strongly coupled in general and even in response to disturbance (e.g. Nave et al. 2011; Delgado-Baquerizo et al. 2013; Zhou et al. 2018c). More importantly, in contrast to the constrained responses of soil C:N ratio to woody encroachment throughout the soil profile, responses of soil C:P and N:P ratios were relatively more flexible. More specifically, spatial heterogeneities of soil C:P and N:P ratios were substantially higher than those of soil C:N ratios (Fig. 5), and decreasing magnitudes in soil C:P and N:P ratios throughout the soil profile were proportionally more dramatic than those of soil C:N ratios (Tables 1 and 2).

C:N ratios decreased by approximately 20%, while C:P and N:P ratios decreased by 50–80% from the top to the bottom of the soil profile. Interestingly, soil C:P and N:P ratios were higher under woody patches compared to grasslands in the 0–5 cm depth increment, but this pattern was reversed (i.e., lower ratios under woody patches) in subsurface (15–120 cm) soils (Table 2, Fig. 4c and 4d).

Our observation of increased soil C:P and N:P ratios in surface soils following woody encroachment is consistent with a previous study in this site which reported both soil C:P and N:P ratios increased linearly with stand age of woody patches (0–10 cm, Kantola 2012), but is different from studies in South Africa which showed no changes in either soil C:P or N:P ratios in savannas following the encroachment of the N-fixers *Dichrostachys cinerea* (0–10 cm, Blaser et al. 2014) and *Acacia zanzibarica* (0–15 cm, Sitters et al. 2013). This discrepancy may be ascribed to the fact that aforementioned savannas in South Africa show no sign of either N or P limitation (Sitters et al. 2013; Blaser et al. 2014), while our site appears to be P limited based on leaf tissue N: P ratios > 16. This P limitation may lead to a more conservative P use efficiency by increasing P resorption during senescence (Aerts 1996; Güsewell 2004; Lü et al. 2012; Zechmeister-Boltenstern et al. 2015), resulting in less deposition of P into surface soils where litter is concentrated. In addition, fast growing N_2-fixers usually have a higher P requirement (Treseder and Vitousek 2001; Vitousek et al. 2002; Houlton et al. 2008) which may be fulfilled by high rates of phosphatase activity beneath soils of N_2-fixing woody plants (Houlton et al. 2008; Blaser et al. 2014). Amplified resorption and mineralization due to P limitation in this system may lead to a less proportional accumulation of P than C and N in surface soils following woody encroachment, thereby increasing soil C:P and N:P ratios.

The depth distribution of soil C:P and N:P ratios in savanna ecosystems is less studied compared to that of soil C:N ratio. However, the dramatic decrease in soil C:P and N:P ratios throughout the soil profile in this study (Table 1 and 2, Fig. 4 and 5) is consistent with results from a regional study based on 2384 soil profiles in China (Tian et al. 2010) and other studies conducted in a variety of ecosystems (Walker and Adams 1958; Lilienfein et al. 2001; Bing et al. 2016). In this subtropical ecosystem, soil C and N decrease dramatically with soil depth throughout the 1.2-m soil profile (Zhou et al. 2018c), coincident with the exponential decline in organic matter inputs (e.g. fine root biomass) from surface to subsurface soils (Zhou et al. 2018b). In contrast, soil P decreases relatively more slowly compared to C and N throughout the soil profile (Zhou et al. 2018c). This differential decrease in the concentrations of C and N versus P from surface to subsurface soils leads to a dramatic decrease in soil C: P and N: P ratios with increasing soil depth (Walker and Adams 1958; Wood et al. 1984; Tian et al. 2010). Interestingly, soil C:P and N:P ratios underneath groves decreased faster than those underneath clusters and grasslands (Table 2), creating reversed spatial patterns of soil C:P and N:P ratios in subsurface soils compared to those in surface soils (Fig. 4). In this study site, clusters and grasslands occur on soils with a subsurface argillic horizon, whereas groves are present on non-argillic inclusions (Archer 1995; Zhou et al. 2018a). Coarse-textured subsurface soils underneath groves may provide less physical protection of soil organic matter in aggregates (Liao et al. 2006), thereby enabling more rapid mineralization of soil organic matter (Six et al. 2002). Mineralized C and N eventually leave the system through gaseous emissions (e.g. CO_2, NO, NO_x, N_2O, N_2) and/or leaching (NO_3^-), whereas P can be immobilized by plants and/or microbes or precipitated as calcium phosphates in these alkaline calcareous soils (Carreira et al. 2006; Schlesinger and Bernhardt 2013). In this subtropical system, inorganic C concentration in soils underneath groves are up to an order of magnitude higher than those underneath clusters and grasslands (Appendix S7), suggesting greater potential for P accumulation in soils underneath groves through precipitation (Zhou et al. 2018a). For this reason, subsurface soil C:P and N:P ratios underneath groves were significantly lower than those of clusters and grasslands. This inference is indirectly supported by Pearson's correlation analysis indicating that soil C:P and N:P ratios were significantly and negatively correlated with soil pH and inorganic C concentration in subsurface soils (Table 3).

Conclusions

We found that different plant life-forms (woody vs herbaceous) have distinctive leaf and fine root C:N:P stoichiometry in this subtropical savanna. Correspondingly, the encroachment of *P. glandulosa* and other trees/shrubs has dramatically altered soil C:N:P stoichiometry across this landscape and throughout the soil profile. Differences in soil C:N ratios among different landscape elements and different soil depth increments were relatively small, so their spatial patterns were not strongly affected by vegetation patterns. However, large spatial heterogeneities were found for soil C:P and N:P ratios in both horizontal and vertical planes, creating distinct spatial patterns of soil C:P and N:P ratios that strongly resembled the distribution pattern of woody patches. These contrasting patterns suggest that responses of soil C:N ratios to woody encroachment may be constrained by the strong biological relationship between C and N in soil organic matter inputs and losses, resulting in proportional changes of soil C and N after woody encroachment. In contrast, pool sizes of soil P (and therefore C:P and N:P ratios) can be affected not only by organic matter inputs and losses, but also by geochemical processes that influence the retention of P in the soil environment.

Previous studies have suggested that the influence of woody plant encroachment on soil C, N, and P storage and dynamics is highly related to the identity of encroaching species and site-specific soil nutrient status. For this reason, further studies are needed to determine whether the findings documented in this study are general across grasslands, savannas, and drylands in other biogeographic regions. If our results are generalizable to other dryland regions, the dramatic changes in soil C:P and N:P ratios following woody encroachment may indicate that decoupling of the P cycle from the C and N cycles could be more widespread than previously recognized. This decoupling has strong potential to alter C, N, and P biogeochemical processes that are key determinants of the structure and function of dryland ecosystem.

Acknowledgement This research was supported by a Doctoral Dissertation Improvement Grant from the National Science Foundation (DEB/DDIG1600790), USDA/NIFA Hatch Project (1003961), a Howard McCarley Student Research Award from the Southwestern Association of Naturalists, an Exploration Fund Grant from the Explorers Club, and by a Graduate Student Research Grant from Department of Ecosystem Science and Management at Texas A&M University. Yong Zhou was supported by a Sid Kyle Graduate Merit Assistantship from the Department of Ecosystem Science and Management and a Tom Slick Graduate Research Fellowship from the College of Agriculture and Life Sciences, Texas A&M University. We thank Dr. Ayumi Hyodo and Dr. Ryan Mushinski for technical support in the Stable Isotopes for Biosphere Science Lab at Texas A&M University, and David and Stacy McKown for on-site logistics at the La Copita Research Area.

Author contributions YZ, TWB, and XBW designed the research; YZ conducted fieldwork and performed sample processing and statistical analyses; YZ and TWB interpreted the data; YZ wrote the first draft of the manuscript and all authors contributed substantially to revisions.

References

Aerts R (1996) Nutrient resorption from senescing leaves of perennials: are there general patterns? J Ecol 84:597–608

Archer S (1995) Tree-grass dynamics in a *Prosopis*-thornscrub savanna parkland: reconstructing the past and predicting the future. Ecoscience 2:83–99

Bai E, Boutton TW, Wu XB, Liu F, Archer SR (2009) Landscape-scale vegetation dynamics inferred from spatial patterns of soil δ13C in a subtropical savanna parkland. J Geophys Res-Biogeosci. https://doi.org/10.1029/2008JG000839

Bai E, Boutton TW, Liu F, Wu XB, Archer SR (2012) Spatial patterns of soil $\delta^{13}C$ reveal grassland-to-woodland successional processes. Org Geochem 42:1512–1518

Bardgett RD, Wardle DA (2010) Aboveground-belowground linkages: biotic interactions, ecosystem processes, and global change. Oxford University Press, Oxford

Batjes NH (1996) Total carbon and nitrogen in the soils of the world. Eur J Soil Sci 47:151–163

Bing H, Wu Y, Zhou J, Sun H, Luo J, Wang J, Yu D (2016) Stoichiometric variation of carbon, nitrogen, and phosphorus in soils and its implication for nutrient limitation in alpine ecosystem of Eastern Tibetan Plateau. J Soils Sediments 16:405–416

Blaser WJ, Shanungu GK, Edwards PJ, Olde Venterink H (2014) Woody encroachment reduces nutrient limitation and promotes soil carbon sequestration. Ecol Evol 4:1423–1438

Boutton TW, Liao JD (2010) Changes in soil nitrogen storage and $\delta^{15}N$ with woody plant encroachment in a subtropical savanna parkland landscape. J Geophys Res-Biogeosci. https://doi.org/10.1029/2009JG001184

Boutton TW, Archer SR, Midwood AJ, Zitzer SF, Bol R (1998) $\delta^{13}C$ values of soil organic carbon and their use in documenting vegetation change in a subtropical savanna ecosystem. Geoderma 82:5–41

Boutton TW, Archer SR, Midwood AJ (1999) Stable isotopes in ecosystem science: structure, function and dynamics of a

subtropical savanna. Rapid Commun Mass Spectrom 13:1263–1277
Boutton TW, Kantola IB, Stott DE, Balthrop SL, Tribble JE, Filley TR (2009) Soil phosphatase activity and plant available phosphorus increase following grassland invasion by N-fixing tree legumes. EOS Trans Am Geophys Union 90(52):B21B–0338
Brunelle A, Minckley TA, Delgadillo J, Blissett S (2014) A long-term perspective on woody plant encroachment in the desert southwest, New Mexico, USA. J Veg Sci 25:829–838
Carreira JA, Vinegla B, Lajtha K (2006) Secondary CaCO3 and precipitation of P-Ca compounds control the retention of soil P in arid ecosystems. J Arid Environ 64:460–473
Chiti T, Mihindou V, Jeffery KJ, Malhi Y, De Oliveira FL, White LJ, Valentini R (2017) Impact of woody encroachment on soil organic carbon storage in the Lopé National Park, Gabon. Biotropica 49:9–12
Cleveland CC, Liptzin D (2007) C: N: P stoichiometry in soil: is there a "Redfield ratio" for the microbial biomass? Biogeochemistry 85:235–252
Coetsee C, Gray EF, Wakeling J, Wigley BJ, Bond WJ (2013) Low gains in ecosystem carbon with woody plant encroachment in a South African savanna. J Trop Ecol 29:49–60
Cohen J (1988) Statistical power analysis for the behavioural sciences, 2nd edn. L. Erlbaum Associates, Hillsdale
Creamer CA, Filley TR, Boutton TW, Oleynik S, Kantola IB (2011) Controls on soil carbon accumulation during woody plant encroachment: evidence from physical fractionation, soil respiration, and $\delta^{13}C$ of respired CO_2. Soil Biol Biochem 43:1678–1687
Delgado-Baquerizo M, Maestre FT, Gallardo A, Bowker MA, Wallenstein MD, Quero JL et al (2013) Decoupling of soil nutrient cycles as a function of aridity in global drylands. Nature 502:672–676
Devine AP, McDonald RA, Quaife T, Maclean IMD (2017) Determinants of woody encroachment and cover in African savannas. Oecologia 183:939–951
Di Palo F, Fornara DA (2017) Plant and soil nutrient stoichiometry along primary ecological successions: is there any link? PLoS ONE 12(8):e0182569. https://doi.org/10.1371/journal.pone.0182569
Dijkstra FA, Pendall E, Morgan JA, Blumenthal DM, Carrillo Y, LeCain DR, Follett RF, Williams DG (2012) Climate change alters stoichiometry of phosphorus and nitrogen in a semiarid grassland. New Phytol 196:807–815
Dintwe K, Okin GS, D'Odorico P, Hrast T, Mladenov N, Handorean A, Bhattachan A, Caylor KK (2015) Soil organic C and total N pools in the Kalahari: potential impacts of climate change on C sequestration in savannas. Plant Soil 396:27–44
Dutilleul P, Clifford P, Richardson S, Hemon D (1993) Modifying the t test for assessing the correlation between two spatial processes. Biometrics 49:305–314
Elser JJ, Fagan WF, Denno RF, Dobberfuhl DR (2000) Nutritional constraints in terrestrial and freshwater food webs. Nature 408:578–580
Elser JJ, Fagan WF, Kerkhoff AJ, Swenson NG, Enquist BJ (2010) Biological stoichiometry of plant production: metabolism, scaling and ecological response to global change. New Phytol 186:593–608
Ettema CH, Wardle DA (2002) Spatial soil ecology. Trends Ecol Evol 17:177–183
Filley TR, Boutton TW, Liao JD, Jastrow JD, Gamblin DE (2008) Chemical changes to nonaggregated particulate soil organic matter following grassland-to-woodland transition in a subtropical savanna. J Geophys Res-Biogeosci. https://doi.org/10.1029/2007JG000564
Geesing D, Felker P, Bingham RL (2000) Influence of mesquite (*Prosopis glandulosa*) on soil nitrogen and carbon development: implications for global carbon sequestration. J Arid Environ 46:157–180
Güsewell S (2004) N: P ratios in terrestrial plants: variation and functional significance. New Phytol 164:243–266
Han W, Fang J, Guo D, Zhang Y (2005) Leaf nitrogen and phosphorus stoichiometry across 753 terrestrial plant species in China. New Phytol 168:377–385
Harris D, Horwáth WR, van Kessel C (2001) Acid fumigation of soils to remove carbonates prior to total organic carbon or carbon-13 isotopic analysis. Soil Sci Soc Am J 65:1853–1856
Hibbard KA, Archer S, Schimel DS, Valentine DW (2001) Biogeochemical changes accompanying woody plant encroachment in a subtropical savanna. Ecology 82:1999–2011
Houlton BZ, Wang YP, Vitousek PM, Field CB (2008) A unifying framework for dinitrogen fixation in the terrestrial biosphere. Nature 454:327–330
Jackson RB, Canadell J, Ehleringer JR, Mooney HA, Sala OE, Schulze ED (1996) A global analysis of root distributions for terrestrial biomes. Oecologia 108:389–411
Jackson RB, Banner JL, Jobbágy EG, Pockman WT, Wall DH (2002) Ecosystem carbon loss with woody plant invasion of grasslands. Nature 418:623–626
Kantola I (2012) Biogeochemistry of woody plant invasion: phosphorus cycling and microbial community composition. Ph.D. Thesis, Texas A&M University, College Station, TX, USA
Koerselman W, Meuleman AF (1996) The vegetation N: P ratio: a new tool to detect the nature of nutrient limitation. J Appl Ecol 33:1441–1450
Lajtha K, Driscoll CT, Jarrell WM, Elliott ET (1999) Soil phosphorus: characterization and total element analysis. Standard soil methods for long-term ecological research. Oxford University Press, New York, pp 115–142
Liao JD, Boutton TW, Jastrow JD (2006) Storage and dynamics of carbon and nitrogen in soil physical fractions following woody plant invasion of grassland. Soil Biol Biochem 38:3184–3196
Lilienfein J, Wilcke W, Thomas R, Vilela L, do Carmo Lima S, Zech W (2001) Effects of *Pinus caribaea* forests on the C, N, P, and S status of Brazilian savanna Oxisols. For Ecol Manag 147:171–182
Littell RC, Stroup WW, Milliken GA, Wolfinger RD, Schabenberger O (2006) SAS for mixed models. SAS Institute, Cary
Liu F, Wu X, Bai E, Boutton TW, Archer SR (2010) Spatial scaling of ecosystem C and N in a subtropical savanna landscape. Glob Change Biol 16:2213–2223

Liu F, Wu X, Bai E, Boutton TW, Archer SR (2011) Quantifying soil organic carbon in complex landscapes: an example of grassland undergoing encroachment of woody plants. Glob Change Biol 17:1119–1129

Lü XT, Freschet GT, Flynn DF, Han XG (2012) Plasticity in leaf and stem nutrient resorption proficiency potentially reinforces plant–soil feedbacks and microscale heterogeneity in a semi-arid grassland. J Ecol 100:144–150

Manzoni S, Trofymow JA, Jackson RB, Porporato A (2010) Stoichiometric controls on carbon, nitrogen, and phosphorus dynamics in decomposing litter. Ecol Monogr 80:89–106

Manzoni S, Taylor P, Richter A, Porporato A, Ågren GI (2012) Environmental and stoichiometric controls on microbial carbon-use efficiency in soils. New Phytol 196:79–91

McCulley RL, Jackson RB (2012) Conversion of tallgrass prairie to woodland: consequences for carbon and nitrogen cycling. Am Midl Nat 167:307–321

McGill WB, Cole CV (1981) Comparative aspects of cycling of organic C, N, S and P through soil organic matter. Geoderma 26:267–286

McGroddy ME, Daufresne T, Hedin LO (2004) Scaling of C: N: P stoichiometry in forests worldwide: Implications of terrestrial Redfield-type ratios. Ecology 85:2390–2401

Moore TR, Trofymow JA, Prescott TE, Titus BD, CIDET Working Group (2011) Nature and nurture in the dynamics of C, N and P during litter decomposition in Canadian forests. Plant Soil 339:163–175

Mooshammer M, Wanek W, Hammerle I, Fuchslueger L, Hofhansl F, Knoltsch A, Schnecker J, Takriti M, Watzka M, Wild B, Keiblinger KM, Zechmeister-Boltenstern S, Richter A (2014) Adjustment of microbial nitrogen use efficiency to carbon:nitrogen imbalances regulates soil nitrogen cycling. Nat Commun 5:3694. https://doi.org/10.1038/ncomms4694

Morgan JA, Milchunas DG, LeCain DR, West M, Mosier AR (2007) Carbon dioxide enrichment alters plant community structure and accelerates shrub growth in the shortgrass steppe. Proc Natl Acad Sci USA 104:14724–14729

Murphy J, Riley JP (1962) A modified single solution method for the determination of phosphate in natural waters. Anal Chim Acta 27:31–36

Myrold D (2005) Transformations of nitrogen. In: Sylvia DM, Hartel PG, Fuhrmann JJ, Zuberer DA (eds) Principles and applications of soil microbiology. Pearson Prentice Hall, Upper Saddle River, pp 333–372

Nave LE, Gough CM, Maurer KD, Bohrer G, Hardiman BS, Le Moine J, Munoz AB, Nadelhoffer KJ, Sparks JP, Strahm BD, Vogel CS, Curtis PS (2011) Disturbance and the resilience of coupled carbon and nitrogen cycling in a north temperate forest. J Geophys Res Biogeosci 116:G04016. https://doi.org/10.1029/2011JG001758

Peng Y, Niklas KJ, Sun S (2011) The relationship between relative growth rate and whole-plant C: N: P stoichiometry in plant seedlings grown under nutrient-enriched conditions. J Plant Ecol 4:147–156

Plotnick RE, Gardner RH, Hargrove WW, Prestegaard K, Perlmutter M (1996) Lacunarity analysis: a general technique for the analysis of spatial patterns. Phys Rev E 53:54–61

Png GK, Turner BL, Albornoz FE, Hayes PE, Lambers H, Laliberté E (2017) Greater root phosphatase activity in nitrogen-fixing rhizobial but not actinorhizal plants with declining phosphorus availability. J Ecol 105:1246–1255

R Development Core Team (2014) R: a language and environment for statistical computing. Vienna, Austria. http://www.R-project.org

Redfield AC (1958) The biological control of chemical factors in the environment. Am Scientist 46:205–221

Reich PB, Oleksyn J (2004) Global patterns of plant leaf N and P in relation to temperature and latitude. Proc Natl Acad Sci USA 101:11001–11006

Rosenberg MS, Anderson CD (2011) PASSaGE: pattern analysis, spatial statistics and geographic exegesis. Version 2. Methods Ecol Evol 2:229–232

Sardans J, Rivas-Ubach A, Peñuelas J (2012) The C: N: P stoichiometry of organisms and ecosystems in a changing world: a review and perspectives. Perspect Plant Ecol Evol Syst 14:33–47

Schenk HJ, Jackson RB (2002) Rooting depths, lateral root spreads and below-ground/above-ground allometries of plants in water-limited ecosystems. J Ecol 90:480–494

Schlesinger WH, Bernhardt ES (2013) Biogeochemistry, an analysis of global change. Academic Press, San Diego

Schlesinger WH, Raikes JA, Hartley AE, Cross AF (1996) On the spatial pattern of soil nutrients in desert ecosystems. Ecology 77:364–374

Scholes RJ, Archer SR (1997) Tree-grass interactions in savannas. Annu Rev Ecol Syst 28:517–544

Sistla SA, Schimel JP (2012) Stoichiometric flexibility as a regulator of carbon and nutrient cycling in terrestrial ecosystems under change. New Phytol 196:68–78

Sitters J, Edwards PJ, Venterink HO (2013) Increases of soil C, N, and P pools along an acacia tree density gradient and their effects on trees and grasses. Ecosystems 16:347–357

Six J, Conant RT, Paul EA, Paustian K (2002) Stabilization mechanisms of soil organic matter: implications for C-saturation of soils. Plant Soil 241:155–176

Soil Survey Staff (1999) Soil taxonomy: a basic system of soil classification for making and interpreting soil surveys. Second edition. Natural Resources Conservation Service, U.S. Department of Agriculture, Washington, D.C., USA

Soper FM, Boutton TW, Sparks JP (2015) Investigating patterns of symbiotic nitrogen fixation during vegetation change from grassland to woodland using fine scale $\delta^{15}N$ measurements. Plant, Cell Environ 38:89–100

Springsteen A, Loya W, Liebig M, Hendrickson J (2010) Soil carbon and nitrogen across a chronosequence of woody plant expansion in North Dakota. Plant Soil 328:369–379

Sterner RW, Elser JJ (2002) Ecological stoichiometry: the biology of elements from molecules to the biosphere. Princeton University Press, Princeton

Stevens N, Lehmann CE, Murphy BP, Durigan G (2017) Savanna woody encroachment is widespread across three continents. Glob Change Biol 23:235–244

Throop HL, Archer SR (2008) Shrub (*Prosopis velutina*) encroachment in a semidesert grassland: spatial–temporal changes in soil organic carbon and nitrogen pools. Glob Change Biol 14:2420–2431

Tian H, Chen G, Zhang C, Melillo JM, Hall CA (2010) Pattern and variation of C: N: P ratios in China's soils: a synthesis of observational data. Biogeochemistry 98:139–151

Treseder KK, Vitousek PM (2001) Effects of soil nutrient availability on investment in acquisition of N and P in Hawaiian rain forests. Ecology 82:946–954

Van Auken OW (2009) Causes and consequences of woody plant encroachment into western North American grasslands. J Environ Manag 90:2931–2942

Vitousek PM, Cassman K, Cleveland C, Crews T, Field CB, Grimm NB, Howarth RW, Marino R, Martinelli L, Rastetter EB, Sprent JI (2002) Towards an ecological understanding of biological nitrogen fixation. Biogeochemistry 57:1–45

Walker TW, Adams AFR (1958) Studies on soil organic matter: I. Influence of phosphorus content of parent materials on accumulations of carbon, nitrogen, sulfur, and organic phosphorus in grassland soils. Soil Sci 85:307–318

Watts SE (1993) Rooting patterns of co-occurring woody plants on contrasting soils in a subtropical savanna. M.S. Thesis. Texas A&M University, College Station, Texas, USA

Wheeler CW, Archer SR, Asner GP, McMurtry CR (2007) Climatic/edaphic controls on soil carbon/nitrogen response to shrub encroachment in desert grassland. Ecol Appl 17:1911–1928

Whittaker RH, Gilbert LE, Connell JH (1979) Analysis of two-phase pattern in a mesquite grassland, Texas. J Ecol 67:935–952

Wigley BJ, Bond WJ, Hoffman TM (2010) Thicket expansion in a South African savanna under divergent land use: local vs. global drivers? Glob Change Biol 16:964–976

Wood T, Bormann FH, Voigt GK (1984) Phosphorus cycling in a northern hardwood forest: biological and chemical control. Science 223:391–393

Xiao C, Janssens IA, Zhou Y, Su J, Liang Y, Guenet B (2015) Strong stoichiometric resilience after litter manipulation experiments; a case study in a Chinese grassland. Biogeosciences 12:757–767

Yuan ZY, Chen HY, Reich PB (2011) Global-scale latitudinal patterns of plant fine-root nitrogen and phosphorus. Nat Commun 2:344. https://doi.org/10.1038/ncomms1346

Yue K, Fornara DA, Yang W, Peng Y, Li Z, Wu F, Peng C (2017) Effects of three global change drivers on terrestrial C: N: P stoichiometry: a global synthesis. Glob Change Biol. https://doi.org/10.1111/gcb.13569

Zechmeister-Boltenstern S, Keiblinger KM, Mooshammer M, Peñuelas J, Richter A, Sardans J, Wanek W (2015) The application of ecological stoichiometry to plant–microbial–soil organic matter transformations. Ecol Monogr 85:133–155

Zhou Y, Boutton TW, Wu XB (2017a) Soil carbon response to woody plant encroachment: importance of spatial heterogeneity and deep soil storage. J Ecol 105:1738–1749

Zhou Y, Boutton TW, Wu XB, Yang C (2017b) Spatial heterogeneity of subsurface soil texture drives landscape-scale patterns of woody patches in a subtropical savanna. Landsc Ecol 32:915–929

Zhou Y, Boutton TW, Wu XB (2018a) Woody plant encroachment amplifies spatial heterogeneity of soil phosphorus to considerable depth. Ecology 99:136–147

Zhou Y, Boutton TW, Wu XB, Wright CL, Dion AL (2018b) Rooting strategies in a subtropical savanna: a landscape-scale three-dimensional assessment. Oecologia 186:1127–1135

Zhou Y, Boutton TW, Wu XB (2018c) Soil phosphorus does not keep pace with soil carbon and nitrogen accumulation following woody encroachment. Glob Change Biol. 24:1992–2007

Zitzer SF, Archer SR, Boutton TW (1996) Spatial variability in the potential for symbiotic N_2 fixation by woody plants in a subtropical savanna ecosystem. J Appl Ecol 33:1125–1136

Appendix S1

C: N, N: P, and C: P ratios of leaf and fine root tissues for each plant species across this 160 m × 100 m landscape in a subtropical savanna. Number of non N_2-fixing woody species = 13, N_2-fixing woody species = 2, forbs = 9, grasses = 13, and CAM species = 3. N_2-fixing woody species were identified according to Zitzer et al. (1996).

Species name	Leaf tissue				Fine root tissue		
	C: N	N: P	C: P		C: N	N: P	C: P
Non N_2-fixing woody species							
Bernardia myricifolia	14.21	26.39	374.87		25.87	30.67	793.51
Celtis pallida	10.20	34.94	356.28		15.12	97.03	1467.12
Condalia hookeri	22.71	25.82	586.50		19.87	44.18	877.66
Diospyros texana	22.23	28.15	625.60		40.79	32.02	1306.29
Foresteria angustifolia	21.92	25.49	558.67		47.74	18.73	894.29
Karwinskia humboldtiana	16.37	28.55	467.24		46.15	19.92	919.49
Lycium berlandieri	23.44	20.68	484.71		46.41	24.48	1135.95
Mahonia trifoliolata	34.83	16.20	564.33		33.48	37.05	1240.60
Schaefferia cuneifolia	17.27	21.47	370.82		14.96	73.93	1105.92
Zanthoxylum fagara	18.66	21.21	395.87		21.71	40.27	874.24
Coleogyne ramosissima	19.97	24.55	490.18		32.83	57.71	1894.77
Salvia ballotiflora	19.05	17.99	342.69		43.58	26.02	1133.64
Acacia greggii	16.89	26.87	453.91		40.50	51.91	2102.23
N_2-fixing woody species							
Acacia schaffneri	15.32	28.01	429.04		44.07	33.08	1457.83
Prosopis glandulosa	12.76	26.39	336.70		18.99	41.71	791.91
Forbs							
Croton texensis	15.19	21.41	325.34		101.00	30.73	3103.38
Wedelia texana	16.10	22.48	361.95		65.79	29.42	1935.62
Aphanostephus riddellii	19.41	19.18	372.24		53.89	24.16	1301.84
Ambrosia confertiflora	15.30	16.92	258.84		36.90	31.24	1152.69
Parthenium hysterophorus	12.73	41.38	526.75		72.92	21.00	1531.18
Palafoxia callosa	20.43	26.42	539.76		123.40	14.23	1756.25
Amphiachyris amoena	18.63	19.52	363.61		80.27	19.01	1525.79

Thymophylla pentachaeta	20.17	17.99	362.74		69.46	18.70	1298.78
Xanthisma texanum	17.64	23.63	416.67		43.01	18.48	794.68
Grasses							
Tridens albescens	23.88	26.47	632.16		62.95	29.73	1871.67
Setaria texana	12.57	19.96	250.82		34.76	35.53	1235.06
Bothriochloa ischaemum	30.67	15.66	480.38		155.40	22.34	3472.00
Aristida purpurea	33.33	13.06	435.21		120.63	30.96	3734.41
Cenchrus ciliaris	17.20	17.06	293.44		76.52	28.23	2159.82
Heteropogon contortus	29.27	21.56	631.12		157.21	20.25	3182.86
Chloris cucullata	25.77	23.94	617.02		108.19	26.24	2838.57
Eragrostis secundiflora	27.65	20.88	577.40		102.39	32.11	3287.17
Paspalum setaceum	24.02	19.10	458.87		74.91	21.07	1577.96
Sporobolus neglectus	21.90	16.93	370.61		109.64	18.57	2035.91
Bouteloua rigidiseta	28.70	25.81	740.86		115.77	27.37	3168.60
Bouteloua trifida	21.49	17.79	382.29		74.31	27.28	2027.32
Panicum hallii	22.12	26.10	577.11		91.25	25.38	2315.87
CAM species							
Opuntia engelmannii	46.41	17.84	828.15		56.30	31.13	1752.70
Cylindropuntia leptocaulis	41.29	17.81	735.39		43.45	37.37	1623.70
Yucca treculeana	23.97	13.53	324.36		127.23	25.47	3240.55

Reference

Zitzer SF, Archer SR, Boutton TW (1996) Spatial variability in the potential for symbiotic N_2 fixation by woody plants in a subtropical savanna ecosystem. J Appl Ecol 33:1125-1136

Appendix S2

Variogram analyses were used to determine the spatial structure for soil C: N. N: P and C: P ratios along the soil profile. The experimental semivariogram for soil C: N. N: P and C: P ratios in each depth increment was calculated according to:

$$\gamma(h) = \frac{1}{2N(h)} \sum_{i=1}^{i=N(h)} [Z(X_i) - Z(X_{i+h})]^2$$

where $\gamma(h)$ is semivariance and h is the lag distance. $Z(X_i)$ and $Z(X_{i+h})$ are the values of measured properties at a spatial location X_i and X_{i+h}. N(h) is the number of pairs with lag distance h. A spherical model was fitted to each experimental semivariogram to obtain the nugget (C_0), range, partial sill (C), and sill (C_0+C) (see figure). All variogram calculations were conducted using R statistical software (R Development Core Team 2014), and results are shown in Appendix S3, S4, and S5.

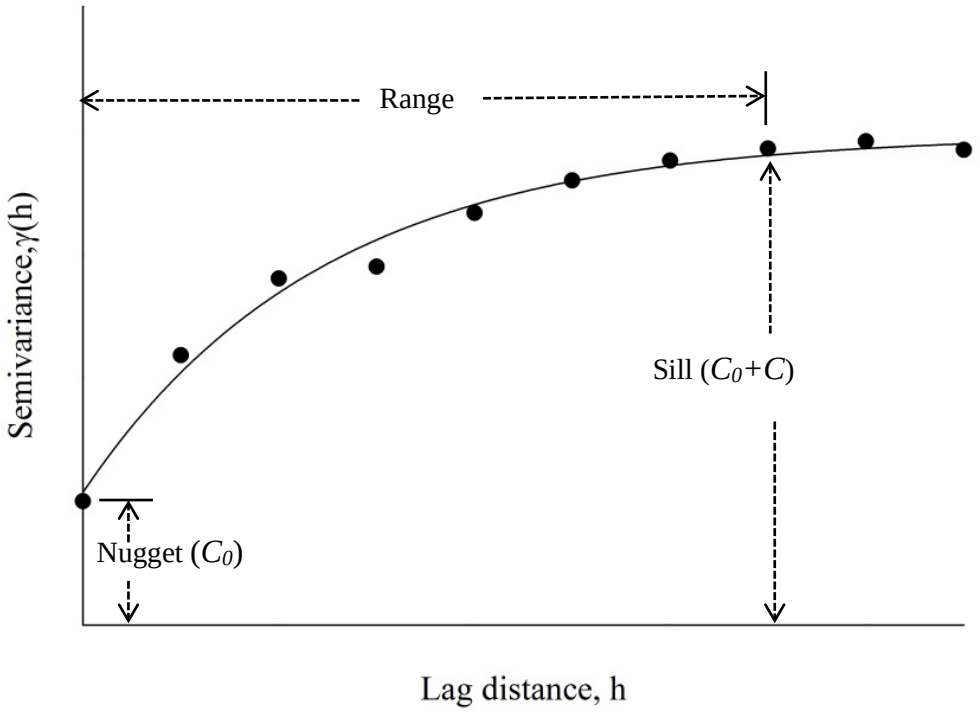

Generalized semivariogram, showing semivariance estimates for observed distance classes (filled circles) and the fitted model (solid line).

Reference

R Development Core Team. 2014. R: A Language and Environment for Statistical Computing. Vienna, Austria. http://www.R-project.org.

Appendix S3

Semivariograms for soil C: N ratios by soil depth based on 320 random soil samples taken across this 160 m × 100 m landscape throughout the soil profile. All semivariograms were constructed using 4 m lag intervals to a maximum lag of 60 m and fitted with spherical models.

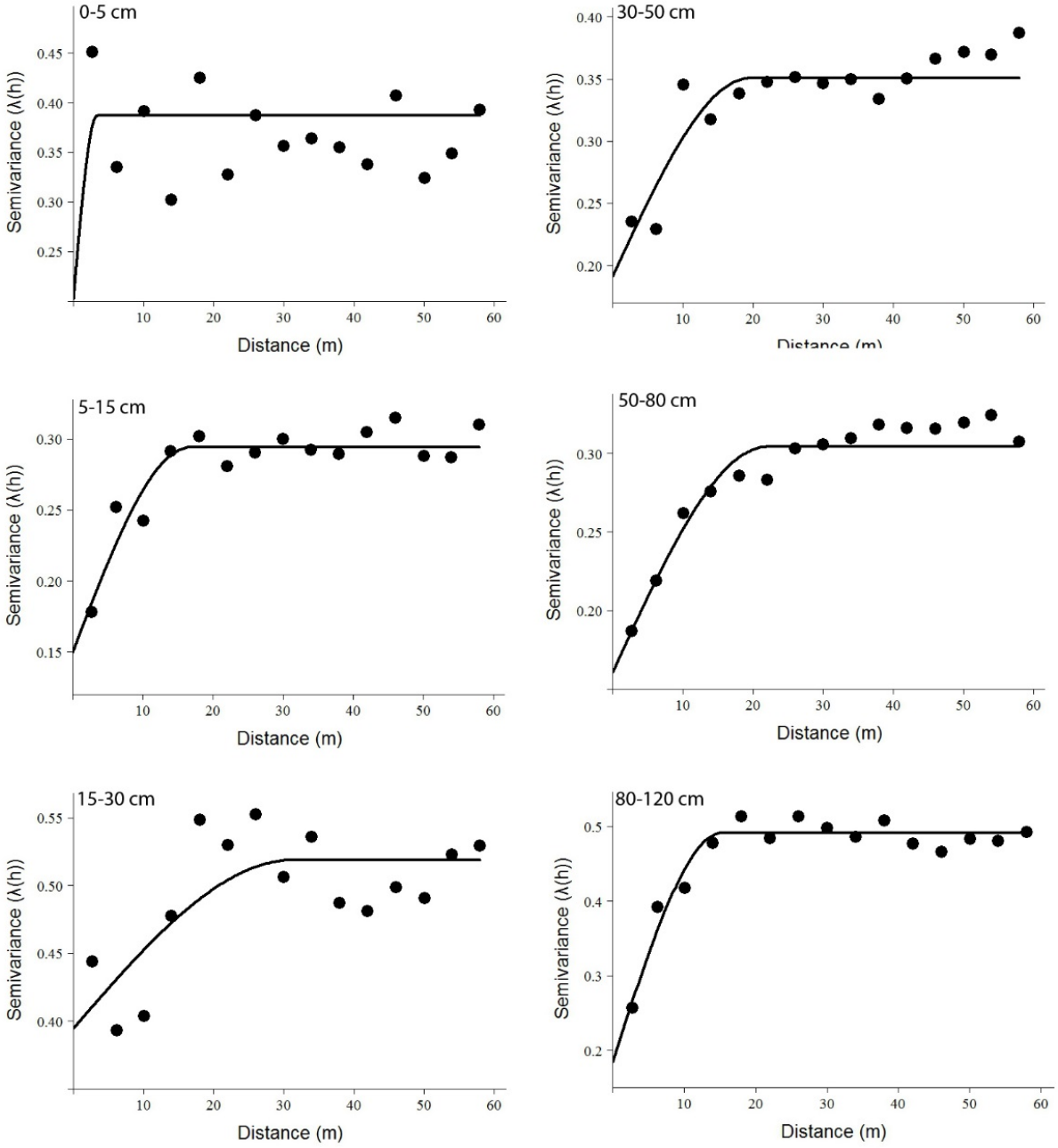

Appendix S4

Semivariograms for soil N: P ratios by soil depth based on 320 random soil samples taken across this 160 m × 100 m landscape throughout the soil profile. All semivariograms were constructed using 4 m lag intervals to a maximum lag of 60 m and fitted with spherical models.

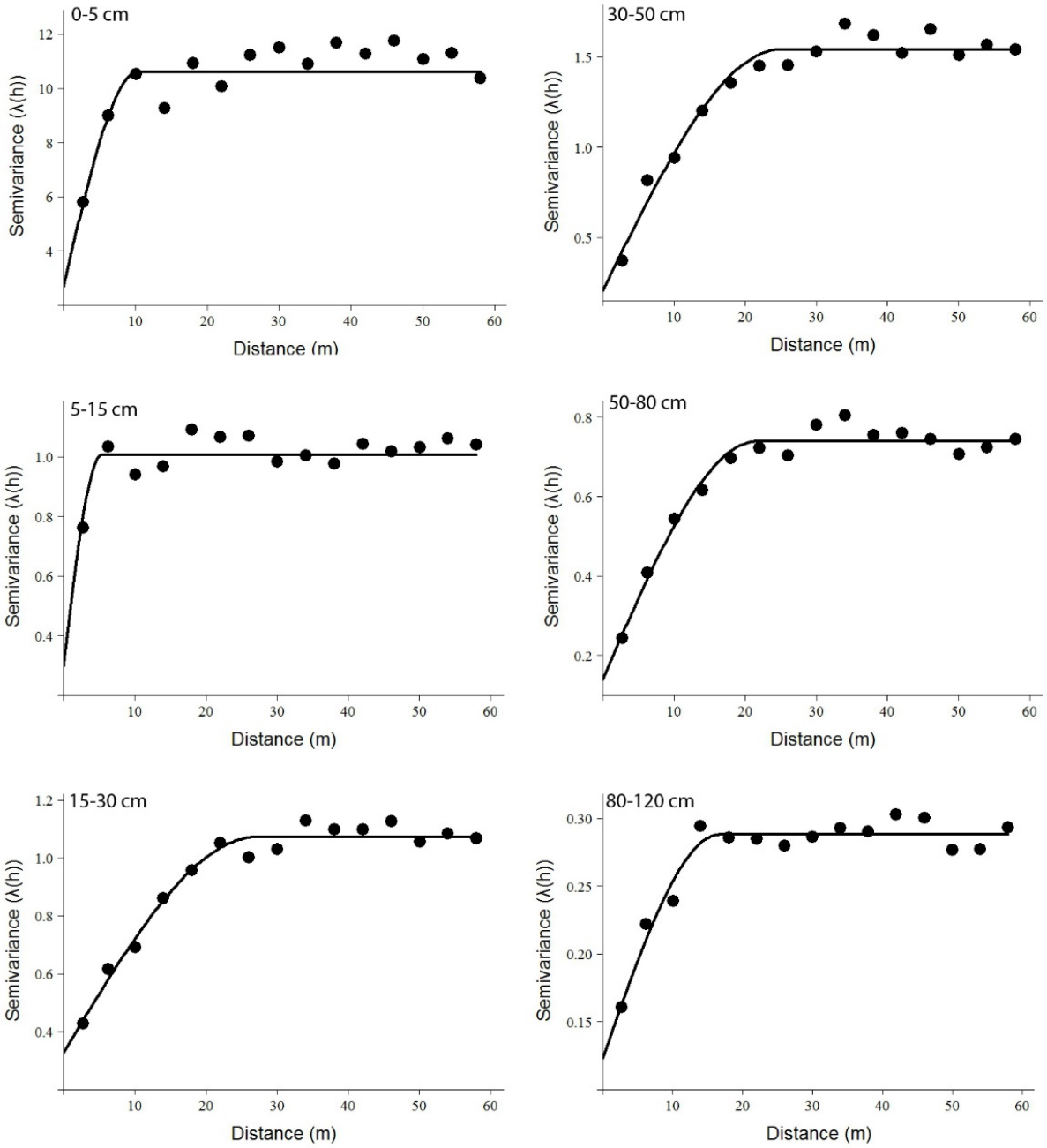

Appendix S5

Semivariograms for soil C: P ratio by soil depth based on 320 random soil samples taken across this 160 m × 100 m landscape throughout the soil profile. All semivariograms were constructed using 4 m lag intervals to a maximum lag of 60 m and fitted with spherical models.

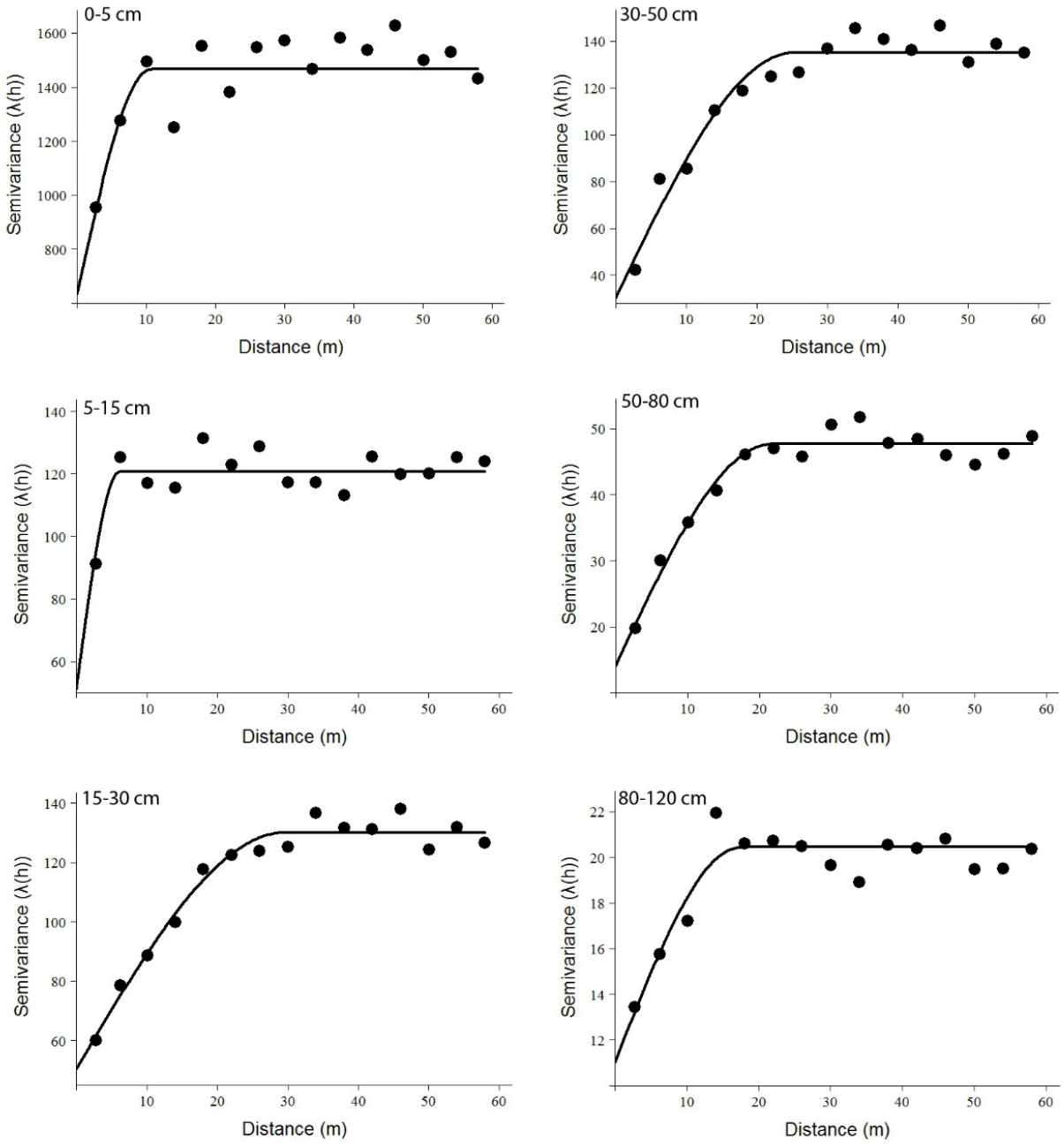

Appendix S6

Parameters for semivariogram of soil C: N, N: P, and C: P ratios based on soil samples taken across this 160 m × 100 m landscape throughout the soil profile.

	Depth (cm)	Nugget (C_0)	Partial sill (C)	Sill (C_0+C)	C/(C_0+C) (%)	Range (m)	R^2	RMSD
C: N ratio	0-5	0.20	0.18	0.38	47.37	3.36	0.02	0.64
	5-15	0.15	0.14	0.29	48.28	16.7	0.15	0.51
	15-30	0.39	0.12	0.51	23.53	31.22	0.16	0.66
	30-50	0.19	0.16	0.35	45.71	19.16	0.23	0.56
	50-80	0.16	0.14	0.30	46.67	22.01	0.55	0.58
	80-120	0.18	0.31	0.49	63.27	15.42	0.16	0.65
N: P ratio	0-5	2.67	7.93	10.60	74.81	10.37	0.22	3.02
	5-15	0.30	0.71	1.01	70.30	5.32	0.013	1.05
	15-30	0.32	0.75	1.07	70.09	27.20	0.51	0.74
	30-50	0.21	1.34	1.55	86.45	24.93	0.57	0.81
	50-80	0.14	0.60	0.74	81.08	21.69	0.55	0.58
	80-120	0.12	0.17	0.29	58.62	16.74	0.23	0.47
C: P ratio	0-5	633.61	831.94	1465.55	56.77	10.66	0.19	36.51
	5-15	51.28	69.42	120.70	57.51	6.20	0.018	11.51
	15-30	50.35	79.72	130.07	61.29	29.67	0.45	8.52
	30-50	30.40	104.62	135.02	77.48	25.15	0.49	8.25
	50-80	14.14	33.53	47.67	70.34	21.73	0.46	5.11
	80-120	11.04	9.40	20.44	45.99	17.52	0.16	4.10

RMSD represents the root-mean-square deviation.

Appendix S7

Inorganic carbon concentrations (g C kg^{-1}) for different landscape elements throughout the soil profile. The box plots summarize the distribution of points for inorganic carbon concentration within each landscape element throughout the soil profile. The central box shows the inter-quartile range, median (horizontal solid line in the box), and mean (horizontal dotted line). Lower and upper error bars indicate 10^{th} and 90^{th} percentiles, and points above and below the error bars are individuals above 90^{th} or below 10^{th} percentiles. Number of samples: grassland = 200, cluster = 41, and grove = 79. Significant differences among different landscape elements within each depth increment are indicated with different letters based on Tukey HSD test after One-way ANOVA. Note: scales are different.